



ISSN 0975-413X
CODEN (USA): PCHHAX

Der Pharma Chemica, 2016, 8(2):114-133
(<http://derpharmachemica.com/archive.html>)

Experimental and theoretical study of new synthesized organic compounds on corrosion behaviour and the inhibition of carbon steel in hydrochloric acid solution

M. Larouj¹, M. Belkhaouda², H. Lgaz^{1,2}, R. Salghi^{2,*}, S. Jodeh^{3,*}, S. Samhan⁴, H. Serrar⁵, S. Boukhris⁵, M. Zougagh^{6,7} and H. Oudda¹

¹Laboratory separation processes, Faculty of Science, University Ibn Tofail, Kenitra, Morocco

²Laboratory of Applied Chemistry and Environment, ENSA, Université Ibn Zohr, Agadir, Morocco

³Department of Chemistry, An-Najah National University, Nablus, Palestine

⁴Palestine Water Authority, Ramallah, Palestine

⁴Laboratory of Organic, Organometallic and Theoretical Chemistry, Faculty of Science, Ibn Tofail University, Kenitra, Morocco

⁶Regional Institute for Applied Chemistry Research, IRICA, E-13004, Ciudad Real, Spain

⁷Castilla-La Mancha Science and Technology Park, E-02006, Albacete, Spain

ABSTRACT

The inhibition effect of 8-(4-chlorophenyl)-3-hydroxy-4,6-dioxo-2-(p-toly)-4,6-dihydropyrimido [2,1-b] [1,3] thiazine-7-carbonitrile (HPDTC-1), 3-hydroxy-4,6-dioxo-8-phenyl-2-(p-toly)-4,6-dihydropyrimido [2,1-b] [1,3] thiazine-7-carbonitrile (HPDTC-2) and 3-hydroxy-8-(4-nitrophenyl)-4,6-dioxo-2-(p-toly)-4,6-dihydropyrimido [2,1-b] [1,3] thiazine-7-carbonitrile (HPDTC-3) on the corrosion behavior of carbon steel in hydrochloric solution were investigated by experimentally using polarization, electrochemical impedance spectroscopy and gravimetric measurements and complementary with density functional theory (DFT) methods. The results of this study show that these compounds give excellent inhibiting properties for carbon steel corrosion in acidic medium with the efficiency that exceeds 96% for HPDTC-3, 95% for HPDTC-2 and 92% for HPDTC-1 at 10^{-3} mol/L. Polarization curves prove that these organic compounds act as inhibitors mixed-type. The adsorption of all studied inhibitors on the carbon steel surface follows Langmuir isotherm model. The variation of corrosion currents at different temperatures we lead to determination of activation parameters of the dissolution process and from the Langmuir adsorption isotherm we have calculate the thermodynamic adsorption parameters of the tested inhibitors. For establish the correlation between experimental data and theoretical results, some quantum chemical parameters for the three compounds were evaluated for provide more idea on the mechanism of inhibition of the corrosion process.

Keywords: Corrosion inhibition, HPDTC, polarization curves, EIS and gravimetric methods.

INTRODUCTION

Iron and its alloys plays primordial role in construction materials, which is widely worn in most of the major industries. Acid solutions are generally used in the pickling of iron alloys in industrial processes scale [1-3]. Consequently, in these environments it undergoes certain type of phenomenon corrosion. The addition of organic compounds in an aggressive environment as corrosion inhibitors in order to minimize or prevent corrosion of metals and alloys remain the most efficient method against the corrosion phenomenon. The inhibition investigation of dissolution processes by organic substances has been the subject of several researches [4-6]. The results of these studies confirm that the inhibition effect principally depends to adsorptions centers of inhibitory molecules which heteroatoms and aromatic rings in their structure [7-10]. The adsorption of these inhibitors on the metal surface for

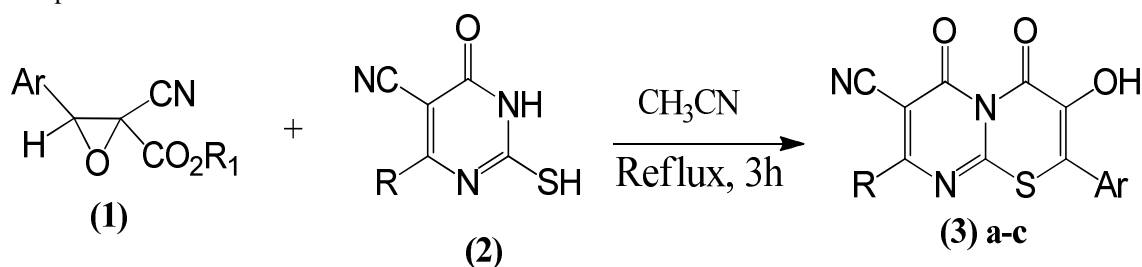
protect the metal surface from the corrosive medium depends on nature and charge of the metal, the type of electrolyte, and the inhibitor structure [11]. Bahrami and co-workers studied the effect of three organic compounds containing nitrogen, oxygen and aromatic rings on the behavior of carbon steel in acidic medium. They concluded that the studied compounds are effective inhibitors at low concentrations [12]. Xu concluded of their experimental study of corrosion inhibition of 3-pyridinecarboxamide thiosemicarbazone for carbon steel in hydrochloric acid that this compound exhibited good inhibition effect and corrosion process was minimized via forming a good molecular film on the carbon steel surface, then decreasing the interaction between metal and the aggressive medium [13]. In the present study, different techniques such as weight loss, polarization, and electrochemical impedance spectra (EIS) were used for evaluate the effect of synthesized organic compounds on the inhibition behavior of carbon steel in 1.0 M HCl. This study was completed using scanning electron microscope (SEM) and quantum chemical calculation.

MATERIALS AND METHODS

2.1. Synthesis

General procedure for the Synthesis of 3-hydroxy-4, 6-dioxo pyrimido[2,1-b][1,3]thiazine-7-carbonitrile:

To a solution of epoxide (1) (1mmol) in acetonitrile (20ml), pyrimidin-4-one derivatives(2) (1mmol) was added, and the mixture was refluxed for 3h. The reaction mixture was distilled using rotary vacuum evaporator to afford crude product, which was treated with a mixture of ether/petroleum ether, the 3-hydroxy-4,6-dioxo-pyrimido[2,1-b][1,3]thiazine-7-carbonitriles **3 a-c** was precipitated and recrystallized from EtOH [14]. Epoxide (1) was prepared in a two-step procedure: the first one is a Knoevenagel-Cope condensation, and the second step is a stereo specific epoxidation of olefin by sodium hydrochlorite [15-16]. All products were characterized by ¹H NMR, ¹³C NMR, IR, and HRMS spectra.



(3)-a Ar: 4-MeC₆H₄ / R₁: CO₂Et / R: 4-ClC₆H₄

(3)-b Ar: 4-MeC₆H₄ / R₁: CO₂Et / R: 4-C₆H₅

(3)-c Ar: 4-MeC₆H₄ / R₁: CO₂Et / R: 4-NO₂C₆H₄

Scheme: An easy, fast, and cheap way for the synthesis of the new 4,6-dioxo-pyrimido[2,1-b][1,3]thiazine-7-carbonitriles using epoxides α -functionalized

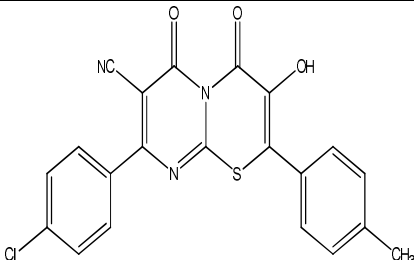
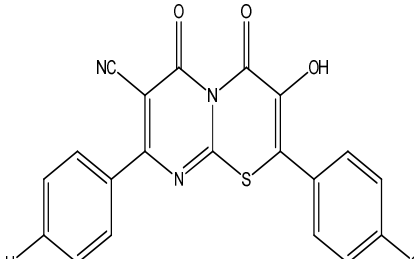
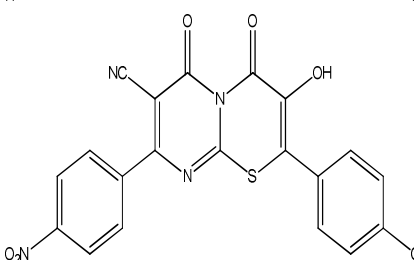
Melting points were taken on a KOFLER hot stage apparatus and are uncorrected. The ¹H NMR spectra were measured in DMSO-d₆ solutions on a Bruker 300 MHz spectrometer using TMS as an internal reference (chemical shift in δ ppm), ¹³C NMR spectra were recorded at 75 MHz. Infrared spectra were carried out on a Tensor 27 spectrometer using KBr pellets. HRMS analyses were carried out using TOF-MS or GCTTOF instrument. IUPAC name, chemical structure and molecular formula, melting point, analytical data and chemical abbreviation of synthesized compounds are given in Table 1.

2.2. Work electrode and electrolyte

The corrosive medium used for all experiments is hydrochloric acid solution of concentration equal to 1.0 M prepared by dilution of an analytical grade 37% HCl with deionized water. The concentration for each tested inhibitor varying from 10⁻⁶ to 10⁻³ mol/L. The carbon steel specimens employed in this study possess the following composition: 0.370 % C, 0.230 % Si, 0.680 % Mn, 0.016 % S, 0.077 % Cr, 0.011 % Ti, 0.059 % Ni, 0.009 % Co, 0.160 % Cu, and Fe balance.

The carbon steel samples used for electrochemical tests were covered in epoxy resin with an exposed surface of 0.5 cm² to the corrosive medium, for gravimetric measurement the coupons with dimensions of 2.5 cm x 2.5 cm x 0.5 cm were employed. Prior to each experiment, a freshly prepared solution was used and the sample was mechanically abraded with different emery papers up to 1200 grade, washed with double distilled water followed by acetone and finally dried in room temperature.

Table 1. IUPAC name, molecular structure, molecular formula, melting point and analytical data of studied HPDTCs

Name of inhibitor	Chemical structure	Molecular formula and m.p
8-(4-chlorophenyl)-3-hydroxy-4,6-dioxo-2-(p-tolyl)-4,6-dihydropyrimido [2,1-b] [1,3] thiazine-7-carbonitrile (HPDTC-1)		$C_{20}H_{12}N_3O_3S$ Mp: >260°C; IR: 1722, 1663, 2222 cm^{-1} . 1H NMR (DMSO-d ₆): δ 7.20–8.35 (m, 8H, Ar), 2.23 (s, 3H, CH ₃ Ar), 13.40 (s, 1H, OH). ^{13}C NMR (DMSO-d ₆): δ 127.4, 129.4, 129.6, 132.1, 139.0, 142.2, 150.2, 167.4 (Ar-C and Csp ²), 163.4 (CO), 166.6 (CO), 115.6 (CN), 21.3 (CH ₃ Ar).
3-hydroxy-4,6-dioxo-8-phenyl-2-(p-tolyl)-4,6-dihydropyrimido [2,1-b] [1,3] thiazine-7-carbonitrile (HPDTC-2)		$C_{20}H_{13}N_3O_3S$ Mp: 199–200°C; IR: 1728, 1667, 2221 cm^{-1} . 1H NMR (DMSO-d ₆): δ 7.198.31 (m, 8H, Ar), 2.23 (s, 3H, CH ₃ Ar), 13.40 (s, 1H, OH). ^{13}C NMR (DMSO-d ₆): δ 128.8, 129.2, 129.6, 132.4, 139.4, 142.8, 150.4, 167.5 (Ar-C and Csp ²), 163.2 (CO), 166.9 (CO), 115.7 (CN), 21.3 (CH ₃ Ar). HRMS calcd. For $C_{21}H_{13}N_3O_3S$ (M+): 387.0675; found: 387.0680.
3-hydroxy-8-(4-nitrophenyl)-4,6-dioxo-2-(p-tolyl)-4,6-dihydropyrimido [2,1-b] [1,3] thiazine-7-carbonitrile (HPDTC-3)		$C_{20}H_{12}N_4O_5S$ Mp: 240–241°C; IR: 174, 1660, 2222 cm^{-1} . 1H NMR (DMSO-d ₆): δ 7.32–7.80 (m, 8H, Ar), 13.40 (s, 1H, OH). ^{13}C NMR (DMSO-d ₆): δ 122.2, 126.3, 127.2, 128.6, 129.3, 131.2, 132.5, 137.9, 142.6, 150.3, 167.4 (Ar-C and Csp ²), 162.8 (CO), 167.5 (CO), 115.3 (CN).

2.3. Electrochemical Measurements

A Potentiostat / Galvanostat PGZ 100 with Voltmaster 4 software are used for the electrochemical impedance spectra and polarization techniques using three electrode cell in which the reference electrode is a saturated calomel electrode (SCE), the counter electrode made of platinum and the working electrode is carbon steel. After stabilization of studied system at open-circuit potential during 30 min immersion, the electrochemical impedance spectroscopy tests were realized at free potential in the frequency range of 100 kHz to 10 mHz with amplitude of the voltage perturbation is 5 mV AC. For potentiodynamic polarization tests, the electrochemical behavior of carbon steel specimen in the corrosive medium in the presence and absence of inhibitor was performed by scanning the potential from –800 to –200 mV/SCE with a scan rate of 1 mV/s.

2.4. Weight loss measurements

The prepared carbon steel electrodes were immersed in aggressive solution with and without the addition of different concentrations of each inhibitor at fixed immersion time of 6 h at 303 K. For each condition, triplicate experiments were performed and the reported weight losses are calculated by average values. For weighing accurately the samples after and before immersion the digital balance with high sensitivity is used.

2.5. Theoretical calculations

Quantum chemical methods are usually used to explore the relationship between the inhibitor molecular properties and its corrosion inhibition efficiency [17–20]. With these methods, the capability of inhibitor molecules to donate or accept electrons can be predicted with analysis of global reactivity parameters, such as energy gap (ΔE) between HOMO and LUMO, dipole moment (μ), total energy (TE), electron negativity (χ), hardness (η), softness (σ), the fraction of electrons transferred (ΔN), etc.

The quantum chemical calculations were carried out with geometrically optimized molecules using Gaussian03, E.01 package [21]. The molecular structures were optimized using the functional hybrid B₃LYP density function theory (DFT) formalism having electron basis set 6-31G (d, p) for all atoms.

According to Koopman's theorem [22] the ionization potential (IE) and electron affinity (EA) of the inhibitors are calculated using the following equations.

$$IE = -E_{\text{HOMO}} \quad (1)$$

$$AE = -E_{\text{LUMO}} \quad (2)$$

Thus, the values of the electronegativity (χ) and the chemical hardness (η) according to Pearson, operational and approximate definitions can be evaluated using the following relations [23]:

$$\chi = \frac{IE + EA}{2} \quad (3)$$

$$\eta = \frac{IE - EA}{2} \quad (4)$$

The number of transferred electrons (ΔN) was also calculated depending on the quantum chemical method [23-24] by using the equation:

$$\Delta N = \frac{\chi_{\text{Fe}} - \chi_{\text{inh}}}{2(\eta_{\text{Fe}} + \eta_{\text{inh}})} \quad (5)$$

Where χ_{Fe} and χ_{inh} denote the absolute electronegativity of iron and inhibitor molecule η_{Fe} and η_{inh} denote the absolute hardness of iron and the inhibitor molecule respectively. In this study, we use the theoretical value of $\chi_{\text{Fe}} = 7.0 \text{ eV mol}^{-1}$ and $\eta_{\text{Fe}} = 0 \text{ eV mol}^{-1}$, for calculating the number of electron transferred.

RESULTS AND DISCUSSION

3.1. Electrochemical Measurements

3.1.1. Potentiodynamic Polarization Studies

The electrochemical behavior of the carbon steel in molar hydrochloric acid solution containing various concentrations of tested inhibitors such as HPDTC-1, HPDTC-2 and HPDTC-3 are shown in Fig. 1 (a, b and c) respectively. It's clear from Fig.1 that the addition of the molecules inhibitor in the corrosive solution causes a remarkable decrease in the cathodic and anodic Tafel curves indicating the decrease their current densities. The cathodic potential plots present the parallel lines showing that the mechanism of the cathodic reduction reaction of hydrogen is not changed and the evolution of this reaction at the carbon steel surface happen mainly by a charge transfer mechanism. The electrochemical parameters that can be deduced from the Fig1 are the corrosion potential (E_{corr}), corrosion current density (I_{corr}), and cathodic Tafel slope (b_c). These parameters and listed in Table 2. The surface coverage (θ) and the inhibition efficiency ($\eta_{\text{Tafel}} \%$) were determined using the following equations:

$$\eta_{\text{Tafel}} (\%) = \frac{I_{\text{corr}}^0 - I_{\text{corr}}}{I_{\text{corr}}^0} \times 100 \quad (6)$$

$$\theta = \frac{I_{\text{corr}}^0 - I_{\text{corr}}}{I_{\text{corr}}^0} \quad (7)$$

Where I_{corr}^0 and I_{corr} are corrosion current density without and with inhibitor, respectively.

The value of I_{corr} is obtained through extrapolating the cathodic Tafel linear to the corrosion potential.

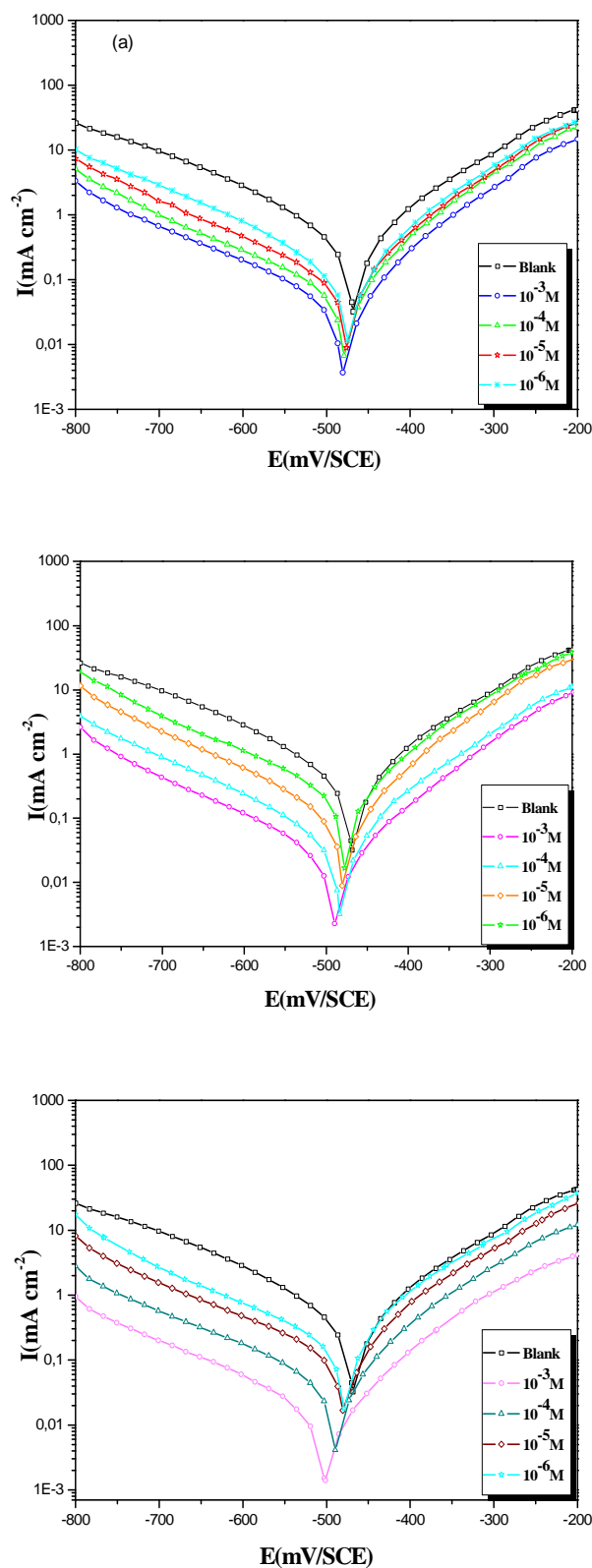


Figure 1. Polarization curves of carbon steel in 1 M HCl for various concentrations of HPDTC-1 (a), HPDTC-2 (b) and HPDTC-3 (c) inhibitors at 303K

Table 2. Electrochemical parameters of carbon steel at various concentrations of compounds in 1.0 M HCl and corresponding inhibition efficiency

Inhibitor	Conc (M)	-E _{corr} (mV/SCE)	-βc (mV dec ⁻¹)	I _{corr} (μA cm ⁻²)	η _{Tafel} (%)	Θ
Blank	1.0	496.0	162.0	564.0	-	-
	10 ⁻³	480.4	192.9	44.49	92.11	0.9211
HPDTC-1	10 ⁻⁴	479.0	187.5	59.16	89.51	0.8951
	10 ⁻⁵	476.5	183.6	121.76	78.41	0.7841
	10 ⁻⁶	474.2	177.2	188.88	66.51	0.6651
	10 ⁻³	489.6	180.9	26.95	95.22	0.9522
HPDTC-2	10 ⁻⁴	483.7	174.4	54.48	90.34	0.9034
	10 ⁻⁵	483.7	174.2	113.47	79.88	0.7988
	10 ⁻⁶	477.8	169.5	177.60	68.51	0.6851
	10 ⁻³	501.7	190.8	17.14	96.96	0.9696
	10 ⁻⁴	489.4	198.8	45.90	91.86	0.9186
HPDTC-3	10 ⁻⁵	480.1	198.2	109.13	80.65	0.8065
	10 ⁻⁶	479.0	187.5	158.14	71.96	0.7196

From the results obtained Fig. 1 and Table 2, we mark that the difference between the corrosion potential (E_{corr}) for uninhibited solution and inhibited solution remains less than 85 mV for all concentrations of three inhibitors. This result shows that, the inhibitors HPDTC-1, HPDTC-2 and HPDTC-3 have the capacity to inhibit both anodic and cathodic reactions; consequently, it can be classed as mixed-type inhibitors [25].

Examination of Table 2 disclose that the values current densities diminish in the order of HPDTC-3 > HPDTC-2 > HPDTC-1. Moreover, the rise of inhibition concentration for the three inhibitors conducts to decrease in I_{corr} value; this can be assigned to excellent surface coverage at higher concentrations of inhibitor.

Evidently, the inhibitory efficiency reaches a much important value equals to 92.11, 95.22 and 96.96 % at same concentration (10⁻³ M) of HPDTC-1, HPDTC-2 and HPDTC-3, respectively, which indicates that the inhibitive capability of HPDTC-3 is far better than other both. This result can be explained by stronger interaction which occurs between the inhibitor molecules and carbon steel because of nitrogen atoms and oxygen in more of electron-rich structure in the molecule of HPDTC-3.

3.1.2. AC Impedance Spectroscopic Studies

Nyquist diagrams recorded at the frequency from 100 Hz to 10 mHz at open circuit potential of carbon steel in corrosive medium without and with different concentrations (10⁻⁶ - 10⁻³ M) of the three inhibitors are shown in Fig. 2 (a, b and c).

The Nyquist plots observed for uninhibited and inhibited solution present a single the capacitive loop which characterize that the process of dissolution metal was mainly controlled by charge transfer. These loops show imperfect semi-circles owing to the phenomenon of dispersing effect which can be related to the roughness and inhomogeneity of the solid surfaces and adsorption of inhibitors [26]

The Nyquist plots were analysed with Zview 2 software by fitting the experimental data to a simple equivalent circuit model [27]. The fitted parameters including; the solution resistance R_s, the charge transfer resistance (R_{ct}) and the constant phase element (CPE) are tabulated in Table 3. The value of double layer capacitance (C_{dl}) may be determined using the following equation:

$$C_{dl} = \sqrt[n]{Q \cdot R_{ct}^{1-n}} \quad (8)$$

The percentage inhibition efficiency calculated from charge transfer resistance across the following equation:

$$\eta_z \% = \frac{(R_{ct} - R_{ct}^0)}{R_{ct}} \times 100 \quad (9)$$

Here R_{ct} and R_{ct}⁰ are the charge transfer resistances in inhibited and uninhibited solutions, respectively. The value of double layer capacitance (C_{dl}) and the inhibitory efficiency are also listed in Table 3.

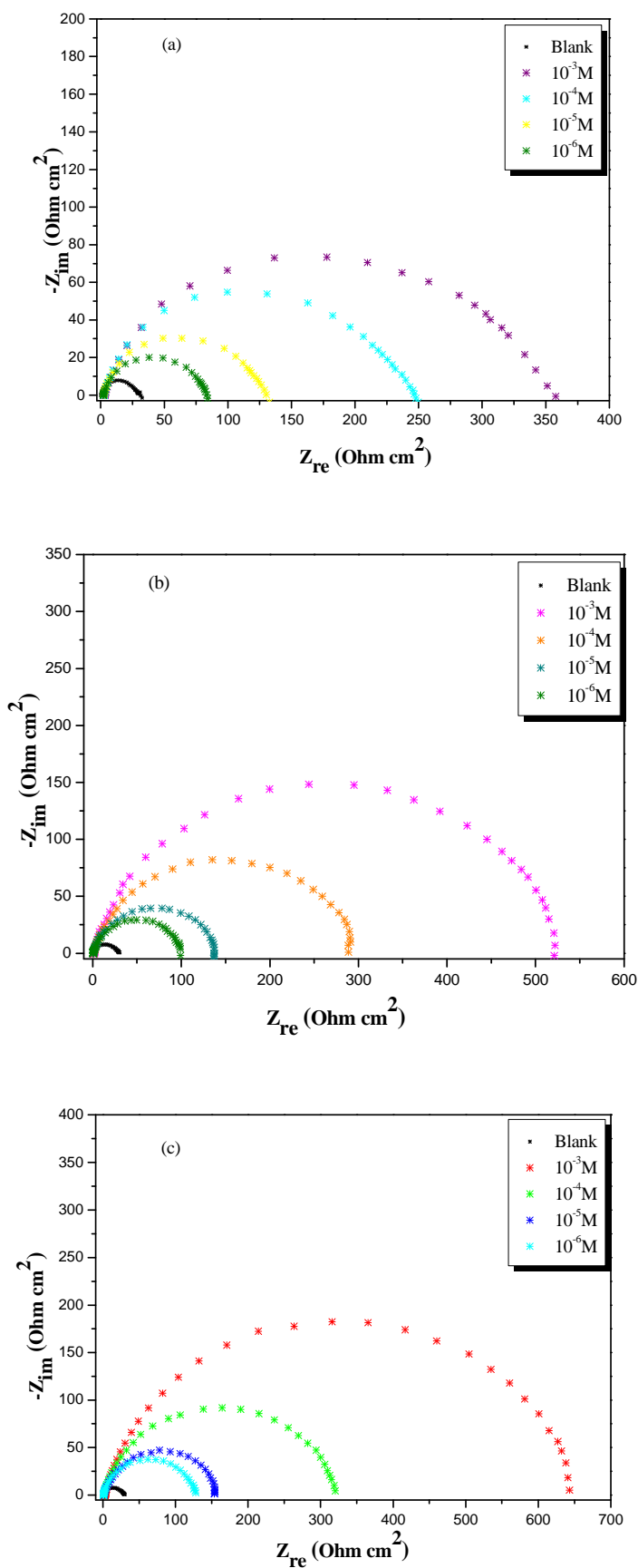


Fig. 2. Nyquist curves for carbon steel in 1M HCl for selected concentrations of HPDTC-1 (a), HPDTC-2 (b) and HPDTC-3 (c) inhibitors 303K

Table 3: Inhibition efficiencies of various concentrations of the inhibitors for corrosion of carbon steel in 1M HCl obtained by EIS measurement at 303K

Inhibitor	Conc (M)	R _{ct} (Ω cm ²)	n	Q×10 ⁻⁵ (s ⁿ Ω ⁻¹ cm ⁻²)	C _{dl} (μF cm ⁻²)	η _a (%)	Θ
Blank	1.0	29.35	0.87	1.7610	80.22	-	-
	10 ⁻³	354.89	0.83	0.53912	22.51	91.73	0.9173
HPDTC-1	10 ⁻⁴	253.89	0.85	0.61445	27.91	88.44	0.8844
	10 ⁻⁵	131.02	0.84	0.96130	38.13	77.60	0.7760
	10 ⁻⁶	84.14	0.87	0.99942	46.53	65.12	0.6512
HPDTC-2	10 ⁻³	513.11	0.88	0.36473	20.33	94.28	0.9428
	10 ⁻⁴	283.02	0.87	0.46759	24.11	89.63	0.8963
	10 ⁻⁵	134.44	0.87	0.65895	32.06	78.17	0.7817
	10 ⁻⁶	99.25	0.88	0.81456	40.34	70.43	0.7043
HPDTC-3	10 ⁻³	640.82	0.87	0.20652	10.22	95.42	0.9542
	10 ⁻⁴	316.27	0.87	0.39137	19.79	90.72	0.9072
	10 ⁻⁵	156.53	0.86	0.56198	24.73	81.25	0.8125
	10 ⁻⁶	125.42	0.89	0.76096	38.57	76.60	0.7660

For the three tested inhibitors, the resistance of charge transfer, R_{ct}, increase gradually with concentration of each inhibitor, which is accompanied of decrease in values of the double layer capacitance C_{dl}, suggests that the adsorption surface increases with concentration of the inhibitors and there by supply excellent barrier towards charge transfer reactions at the metal–solution interface [28].

The inhibition efficiency evaluated from R_{ct} values are established the same trend determined from polarization experiments results which is HPDTC-3 > HPDTC-2 > HPDTC-1.

3.2. Non-Electrochemical Measurements

3.2.1. Weight loss measurements

The effect of addition of HPDTC-1, HPDTC-2 and HPDTC-3 inhibitors on the corrosion behavior of carbon steel in acidic solution was studied by gravimetric measurements at 303K after a 6 h exposure time.

The corrosion inhibition efficiency (η_w%) and the surface coverage (θ) are given by the following relations

$$\eta_w \% = \frac{C_R - C_R^0}{C_R} \times 100 \quad (10)$$

$$\theta = \frac{C_R - C_R^0}{C_R} \quad (11)$$

Where C_R⁰ and C_R are the carbon steel corrosion rates with and without HPDTC-1, HPDTC-2 and HPDTC-3 inhibitor, respectively.

The corrosion rate, the inhibition efficiency, and the surface coverage are presented in Table4.

Table 4: C_R and η_w % obtained from weight loss measurements of carbon steel in 1 M HCl containing various concentrations of inhibitors at different temperatures

Inhibitors	Concentration (M)	C _R (mg cm ⁻² h ⁻¹)	η _w (%)	Θ
Blank	-	1.135	-	-
	10 ⁻³	0.091	91.98	0.9198
HPDTC-1	10 ⁻⁴	0.127	88.81	0.8881
	10 ⁻⁵	0.251	77.88	0.7788
	10 ⁻⁶	0.371	67.31	0.6731
	10 ⁻³	0.057	94.97	0.9497
HPDTC-2	10 ⁻⁴	0.113	90.04	0.9004
	10 ⁻⁵	0.225	80.17	0.8017
	10 ⁻⁶	0.355	68.72	0.6872
	10 ⁻³	0.034	97.01	0.9701
HPDTC-3	10 ⁻⁴	0.105	90.74	0.9074
	10 ⁻⁵	0.221	80.52	0.8052
	10 ⁻⁶	0.331	70.83	0.7083

It is clear from the Table 4 that the corrosion rate decreases and inhibition efficiency with the increase in concentrations of each inhibitor and the inhibition efficiency attained the maximum value of 91.98, 94.97 and 97.01

for HPDTC-1, HPDTC-2 and HPDTC-3 respectively (Fig. 3 and 4). This data confirm those result obtained by the polarization curves and EIS measurements and the better inhibitor for tested serial is HPDTC-3. We can concluded so, that This behavior can be explained based on the strong adsorption of the inhibitor molecules onto the metal surface resulting the presence of heteroatoms N et O and presence of π - electrons.

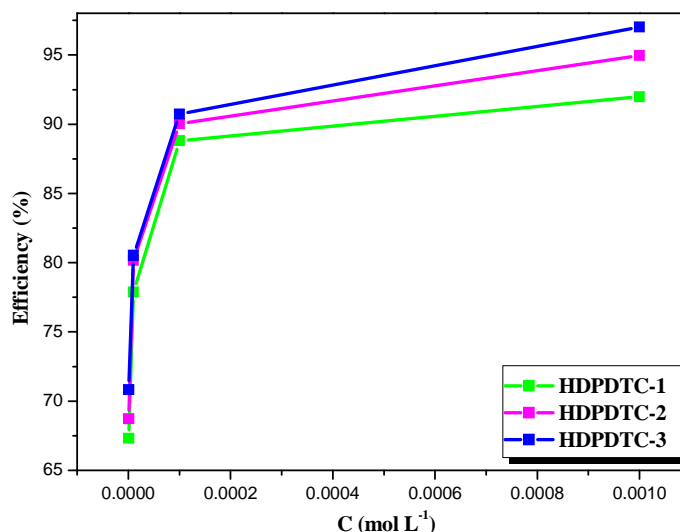


Figure 3. Relationship between the inhibition efficiency and inhibitors concentration for carbon steel after 6 h immersion in 1.0 M HCl at 303 K

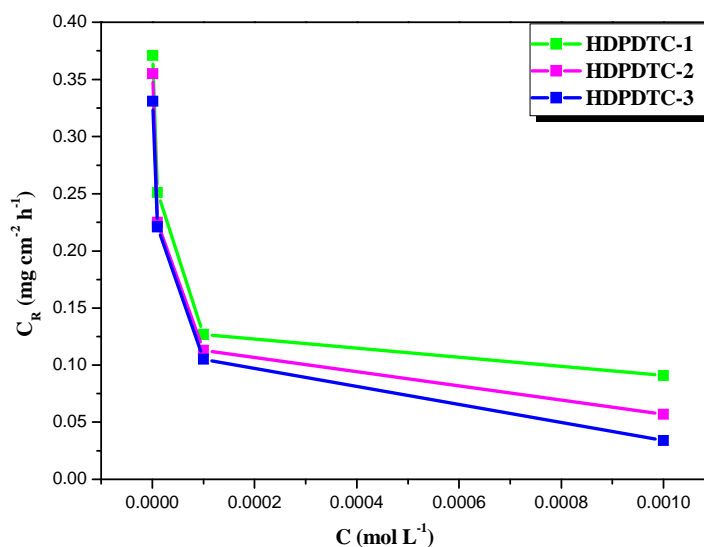


Figure 4. Relationship between the corrosion rate and inhibitors concentrations for steel after 6 h immersion in 1 M HCl at 303 K

3.2.2. Effect of temperature and Kinetic parameters

The temperature effect on the inhibition properties of HPDTC-1, HPDTC-2 and HPDTC-3 inhibitor onto carbon steel electrode were investigated by mass loss experiments in the temperature range 303 to 333K. The corresponding corrosion parameters are exposed in Table 5. It may be distinctly seen from this result that the corrosion rate is more marked with the elevation of temperature for free solution but in the presence of the tested inhibitors, the dissolution rate is extremely reduced. For the same temperature, the increase in the concentration of each inhibitor leads to the elevation the inhibition efficiency values. Nevertheless, for the same concentration of each inhibitor, the properties inhibitory are decreased with increase of temperature.

This result can be attributed to desorption or/and the decrease of the strength of the adsorption process which is caused by increasing the temperature. This behavior reveals is physical adsorption, suggesting physical adsorption mode [29].

The activation thermodynamics parameters of the dissolution process can be determined using Arrhenius Eq. (12) and transition state Eq. (13)

$$C_R = A \cdot \exp\left(-\frac{E_a}{R \cdot T}\right) \quad (12)$$

$$C_R = \frac{RT}{Nh} \cdot \exp\left(\frac{\Delta S_a}{R}\right) \cdot \exp\left(-\frac{\Delta H_a}{RT}\right) \quad (13)$$

where E_a is the apparent activation energy, C_R is the corrosion rate, T is the absolute temperature, R is the universal gas constant, k is the Arrhenius pre-exponential factor, N is the Avogadro's number, h is the Plank's constant, ΔS_a is the activation entropy and ΔH_a is the activation enthalpy.

The graphs of $\ln(C_R)$ against $1/T$ plotted for different concentrations of each inhibitor tested, exposed in Fig. 5 (a, b and c) gives the straight lines with a slope of $(-E_a/R)$. The obtained apparent activation energy E_a in Table 6 reveals that their value in case for inhibited solution is more highly than free solution. This value increases with rising of inhibitor concentration. This behavior can be attributed to an observable diminution in the adsorption of the inhibitor molecules onto the electrode surface with increase in temperature.

The values of enthalpy ΔH_a and entropy ΔS_a of activation for carbon steel corrosion in 1.0 M HCl without and with different concentrations for each organic compounds can be estimated from the slope $(-\Delta H_a/R)$ and intercept $(\log(R/Nh) - (\Delta S_a/R))$ of curves of $\ln(C_R/T)$ versus $1/T$, respectively (Fig. 6 (a, b and c)).

Examinations the results of Table 6 reveal that the value of ΔH_a possesses the positive sign and increase with tested inhibitor concentration. These results reflect the endothermic nature of metal dissolution process suggesting that this dissolution is slowed in the presence of inhibitors and the structure of these compounds affect the force of its adsorption on the metal surface.

It is spotted that the entropy value ΔS_a increases positively with the concentration of the inhibitor. This reflects the formation of an ordered stable film of the inhibitor molecules on the electrode surface. The similar results are obtained by other researchers [30]. The average difference values of the $E_a - \Delta H_a$ obtained in Table 5 allow to check the recognized thermodynamic reaction between this two grandeurs.

Table 5: C_R and η_w % obtained from weight loss measurements of carbon steel in 1 M HCl containing various concentrations of inhibitors at different temperatures

Inhibitors	C (M)	Temperature							
		303 K		313K		323K		333K	
		C_R ($\text{mg cm}^{-2} \text{h}^{-1}$)	η_w (%)	C_R ($\text{mg cm}^{-2} \text{h}^{-1}$)	η_w (%)	C_R ($\text{mg cm}^{-2} \text{h}^{-1}$)	η_w (%)	C_R ($\text{mg cm}^{-2} \text{h}^{-1}$)	η_w (%)
BLANK	1.0	1.135	-	2.466	-	5.032	-	10.029	-
HPDTC-1	10^{-3}	0.091	91.98	0.305	87.63	0.775	84.59	2.063	79.42
	10^{-4}	0.127	88.81	0.389	84.22	0.944	81.24	2.376	76.31
	10^{-5}	0.251	77.88	0.617	74.97	1.471	70.76	3.359	66.51
	10^{-6}	0.371	67.31	0.913	62.97	1.992	60.41	4.581	54.32
HPDTC-2	10^{-3}	0.057	94.97	0.226	90.83	0.564	88.79	1.569	84.35
	10^{-4}	0.113	90.04	0.367	86.11	0.809	83.92	1.999	80.06
	10^{-5}	0.225	80.17	0.582	76.39	1.270	74.76	3.069	69.39
	10^{-6}	0.355	68.72	0.894	63.74	1.859	63.05	4.224	57.88
HPDTC-3	10^{-3}	0.034	97.00	0.118	95.21	0.396	92.13	1.194	88.09
	10^{-4}	0.105	90.74	0.279	88.68	0.728	85.53	1.858	81.47
	10^{-5}	0.221	80.52	0.547	77.81	1.257	75.02	2.949	70.59
	10^{-6}	0.331	70.83	0.771	68.73	1.720	65.82	3.837	61.74

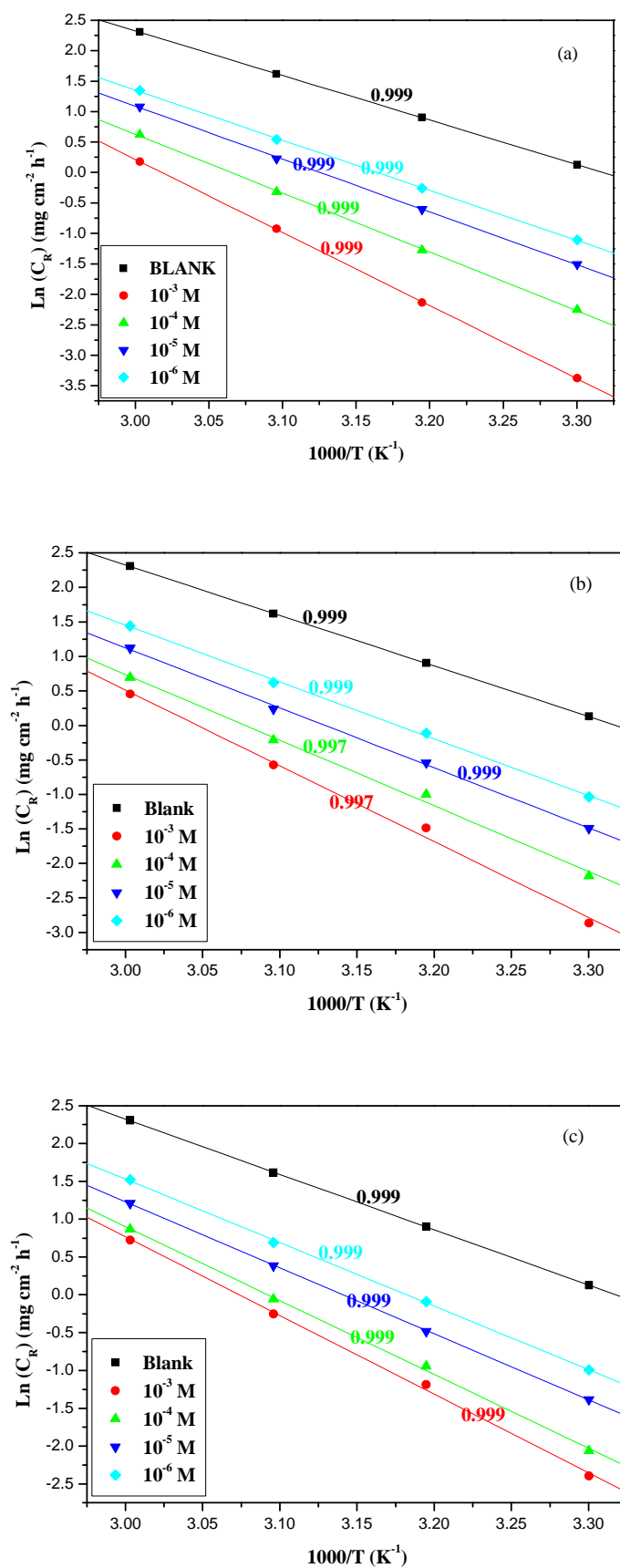
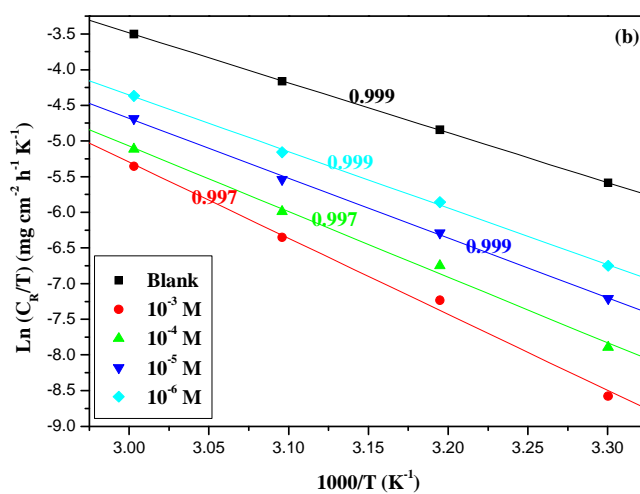
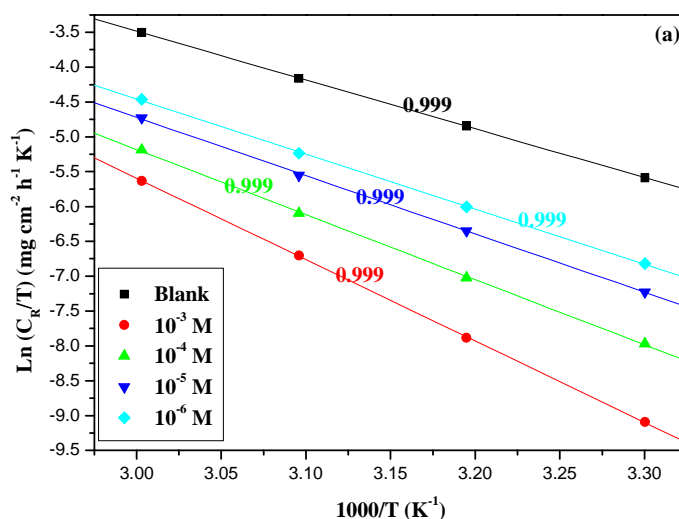


Figure 5. Arrhenius plots for carbon steel in 1 M HCl in the absence and presence of different concentrations of (a) HPDTC-1 (b) HPDTC-2 and (c) HPDTC-3

Table 6. Activation parameters for carbon steel corrosion in 1M HCl in the absence and presence of different concentrations of inhibitors at different temperatures

Inhibitors	Conc. (M)	E _a (kJ mol ⁻¹)	ΔH _a (kJ mol ⁻¹)	ΔS _a (kJ mol ⁻¹ K ⁻¹)	E _a -ΔH _a
Blank	-	60.80	58.16	-51.84	2.64
HPDTC-1	10 ⁻³	99.73	97.09	47.28	2.64
	10 ⁻⁴	80.29	77.65	-7.45	2.64
	10 ⁻⁵	72.14	69.50	-28.08	2.64
	10 ⁻⁶	68.35	65.71	-37.27	2.64
HPDTC-2	10 ⁻³	91.19	88.55	24.28	2.64
	10 ⁻⁴	78.99	76.35	-10.43	2.64
	10 ⁻⁵	72.26	69.62	-27.41	2.64
	10 ⁻⁶	68.44	65.8	-36.14	2.64
HPDTC-3	10 ⁻³	86.4	83.76	12.01	2.64
	10 ⁻⁴	81.16	78.52	-2.56	2.63
	10 ⁻⁵	72.53	69.89	-25.74	2.63
	10 ⁻⁶	69.76	67.12	-31.55	2.64



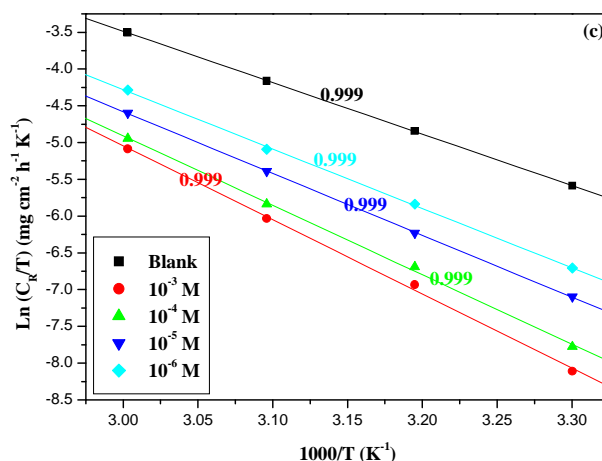


Figure 6. Transition state plots for the inhibition of corrosion of carbon steel in 1M HCl in the absence and presence of different concentrations of (a) HPDTC-1 (b) HPDTC-2 and (c) HPDTC-3

3.2.3. Adsorption Isotherm and thermodynamic parameters

The study of adsorption isotherm is very important for acknowledged the mechanism of corrosion inhibition at the metal/solution interface. The adsorption of organic compound molecules at the carbon steel/solution interface can be considered as a substitution process between the inhibitor molecules in the aqueous solution and the water molecules onto the electrode surface. The adsorption mechanism of different inhibitors on the carbon steel surface was established by fitting the Surface coverage degree (θ) values for different adsorption isotherms at various temperatures. Best fit were granted to Langmuir adsorption isotherm with correlation coefficients close for unity (Fig. 7a, b and c)., According to the isotherm which is related to concentration of inhibitor by:

$$\frac{C_{inh}}{\theta} = \frac{1}{K_{ads}} + C_{inh} \quad (14)$$

Where K_{ads} is the adsorption equilibrium constant of the adsorption process (Fig. 8a, b and c). This constant can be related to the standard free energy of adsorption, ΔG_{ads}^0 , according equation:

$$\Delta G_{ads}^0 = -RT \ln(55.5 K_{ads}) \quad (15)$$

The standard enthalpy of adsorption ΔH_{ads}^0 may be determined using to the Van't Hoff equation (16) or via the Gibbs-Helmholtz equation (17):

$$\ln K_{ads} = -\frac{\Delta H_{ads}^0}{RT} + constant \quad (16)$$

$$\left[\frac{\partial(\frac{\Delta G_{ads}^0}{T})}{\partial T} \right]_P = -\frac{\Delta H_{ads}^0}{T^2} \quad (17)$$

From the curves of $\ln K_{ads}$ versus $1/T$ which have given a straight lines, we can deduced ΔH_{ads}^0 from the slope and the standard entropy of the adsorption process ΔS_{ads}^0 from the intercept of this straight line that is $(\frac{\Delta S_{ads}^0}{R} + \ln \frac{1}{55.5})$. The adsorption parameters of different inhibitors for carbon steel corrosion in 1.0 M HCl at different temperatures are tabulated in Table 7.

The values of adsorption constant K_{ads} calculated for each temperature were found in the order HPDTC-3 > HPDTC-2 > HPDTC-1. The negative sign of ΔG_{ads}^0 proposed that the three inhibitors tested are spontaneously adsorbed on electrode surface. The values of ΔG_{ads}^0 in this study are between -41.99 and 46.56 kJ mol⁻¹ (in Table 7). This result Indicate that the adsorption of these compounds implicates two sorts of interaction, chemisorption more than physisorption. Consequently, we can be concluded that this adsorption is due to the competitive phenomenon between chemical and physical adsorption.

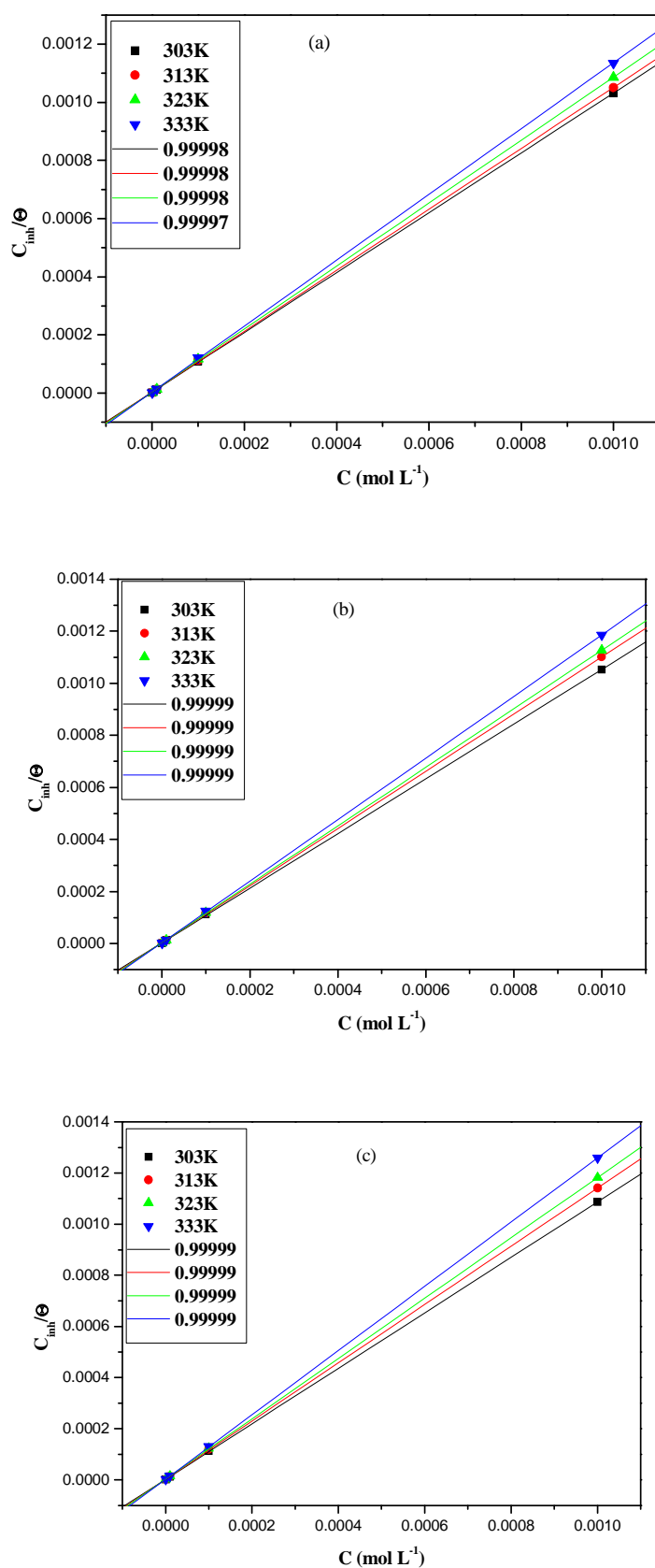


Figure 7. Langmuir adsorption isotherm on carbon steel in 1 M HCl at different temperatures of (a) HPDTC-1 (b) HPDTC-2 and (c) HPDTC-3

Negative sign of ΔH_{ads}^0 reflected the endothermic nature of carbon steel corrosion process. The value of standard enthalpy of adsorption ΔH_{ads}^0 obtained using Van't Hoff equation and that of Gibbs Helmholtz are in good agreement (Fig.9). The large and positive values of ΔS_{ads}^0 indicating that the adsorbed molecules of water onto alloy surface are substituted by the molecules inhibitory which increases the disorder of the solution.

Table 7: Adsorption parameters of inhibitors for carbon steel corrosion in 1M HCl at different temperatures

Inhibitors	Temperature (K)	Langmuir adsorption isotherm		Van't Hoff equation		Gibbs Helmholtz equation
		K_{ads}	ΔG_{ads} (kJ mol ⁻¹)	ΔH_{ads} (kJ mol ⁻¹)	ΔS_{ads} (kJ mol ⁻¹ K ⁻¹)	ΔH_{ads} (kJ mol ⁻¹)
HPDTC-1	303	316021	-41.99		0.11447	
	313	289160	-43.15	-7.30557	0.11451	-7.30556
	323	268845	-44.33		0.11462	
	333	242053	-45.41		0.11442	
HPDTC-2	303	372439	-42.41		0.12542	
	313	351565	-43.66	-4.40670	0.12540	-4.40677
	323	332111	-44.90		0.12536	
	333	318650	-46.18		0.12544	
HPDTC-3	303	479005	-43.04	-7.56691	0.11707	-7.56696
	313	430155	-44.18		0.11697	
	323	390892	-45.34		0.11694	
	333	366319	-46.56		0.11709	

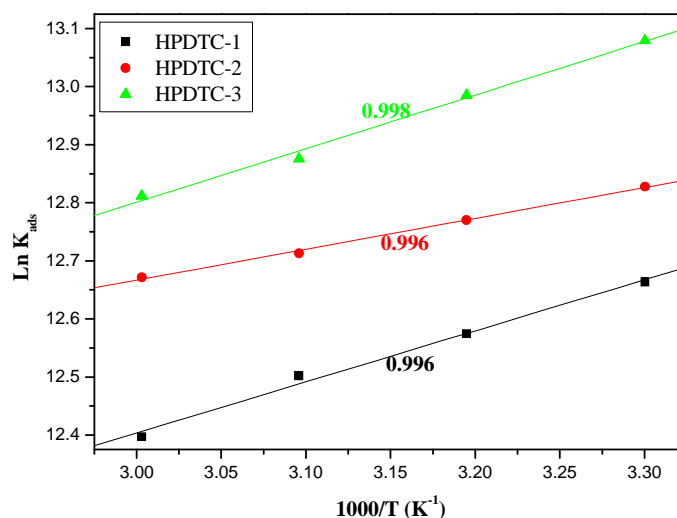


Fig. 8. Plots of Ln K_{ads} Vs $1/T$ for the inhibition of corrosion of carbon steel in 1 M HCl with inhibitors

3.3. DFT method

3.3.1. Molecular geometry

The molecules were built with the Gauss View 3.0 implemented in Gaussian 03 package [21], their corresponding geometries were fully optimized at B3LYP/6-31G (d, p) level of theory in gas phase.

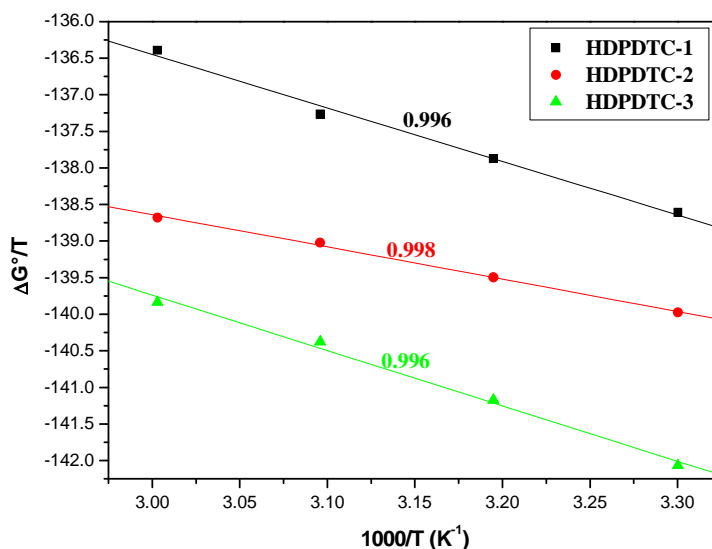


Fig. 9. Plots of $\Delta G^\circ/T$ Vs $1/T$ for the inhibition of corrosion of carbon steel in 1M HCl with inhibitors

Fig. 10 shows the optimized geometry of inhibitors molecule. Frontier orbital density distribution is useful in predicting adsorption centers of the HDPDTCs molecule responsible for the interaction with metal surface atoms. Fig. 10 shows the HOMO and the LUMO density distribution of HDPDTCs. Analysis of Fig. 10 show that the distribution of two energies HOMO and LUMO, we can see that the electron density of the HOMO and LUMO location was distributed almost of the entire molecule and especially the basic skeleton of the molecule that is the bicycle system.

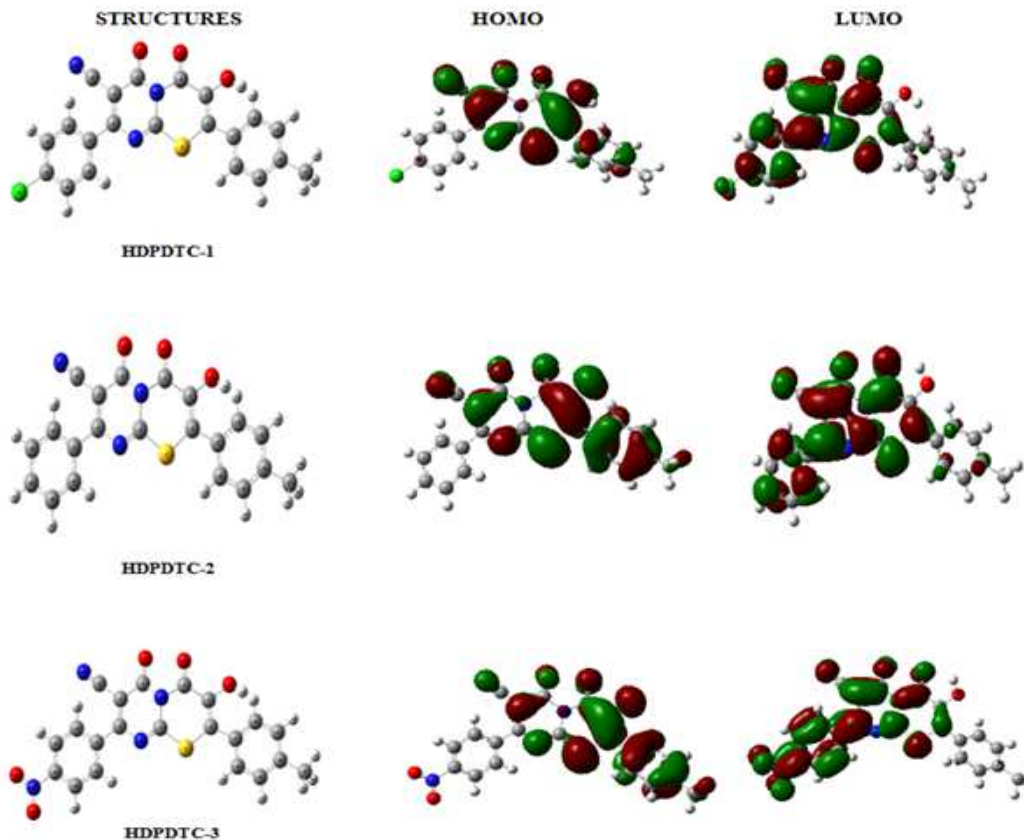
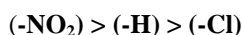


Fig. 10. The optimized molecular structures HOMO and LUMO of the non-protonated inhibitor molecules using DFT/B3LYP/6-31G (d,p)

Table 8. Calculated Quantum Chemical Parameters of the inhibitor molecules

molecule	E_{HOMO} (eV)	E_{LUMO} (eV)	ΔE (eV)	μ (eV)	TE (eV)	η (eV)	σ (eV ⁻¹)	χ (eV)	ΔN	IE (%)
HDPDTC-1	-6.3985	-2.7198	3.6787	12.0333	-55939	1.83935	0.5437	4.5592	0.663	92.11
HDPDTC-2	-6.2417	-2.7892	3.4525	8.8608	-43433	1.72625	0.5793	4.5155	0.719	95.22
HDPDTC-3	-6.4842	-3.3035	3.1807	10.6634	48998	1.59035	0.6288	4.8939	0.662	96.96

The inhibition of steel using substituted pyrimidothiazine as corrosion inhibitors were investigated experimentally. The classification of these inhibitors according to its inhibition efficiency is:



It was found that the ph-NO₂ molecule among the investigated compounds has the highest inhibition efficiency on the metal surface. It is evident to attribute the lower performance of (-NO₂) to the replacement of (-Cl) group by (-NO₂) group. Moreover, the higher inhibition efficiency of (-NO₂) compound than the other inhibitors is probably due to the high polarizability of C-N bond. Also, the higher inhibition efficiency of ph-NO₂ is probably referred to the increasing the number of centers of adsorption on the inhibitor molecules and the higher electron densities caused by the electron releasing (-NO₂) group [23].

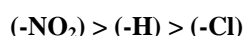
3.3.2. Global molecular reactivity

Frontier orbital theory is useful in predicting adsorption centers of the inhibitor molecules responsible of the interaction metallic surface/molecule [31-33]. The terms involving the frontier molecular orbitals (FMO) could provide dominative contribution, because of the inverse dependence of stabilization energy on orbital energy difference ($\Delta E = E_{\text{LUMO}} - E_{\text{HOMO}}$).

The HOMO energy (E_{HOMO}) is often associated to the electron donating ability of the molecule; therefore, inhibitors with high values of E_{HOMO} have a tendency to donate electrons to appropriate acceptor with low empty molecular orbital energy. Conversely, the LUMO energy (E_{LUMO}) indicates the electron accepting ability of the molecule, the lowest its value the higher the capability of accepting electrons. The gap energy between the frontier orbital's (ΔE) is another important factor in describing the molecular activity, so when the gap energy decreased, the inhibitor efficiency is improved [34].

The calculated quantum chemical parameters related to the inhibition efficiency of the studied molecules, such as the FMO energies (E_{HOMO} , E_{LUMO}), the gap energy (ΔE), the dipole moment (μ), the electro negativity (χ), the ionization potential (IE), the electron affinity (EA), the global hardness (η), and the fraction of electron transfer (ΔN) from the inhibitor molecules to iron, are collected in Table 8.

It was shown from the calculation that (-NO₂) which has the highest inhibition efficiency, has the highest E_{HOMO} . If the energy of HOMO level was decisive for the inhibitor properties, the ranking of the compounds should be:

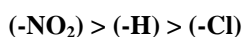


There is an agreement between ranking of E_{HOMO} at B3LYP/6-31G (d, p) level in gas phase and experimental result.

The energy of LUMO indicates the ability of the molecule to accept electrons. So, the lower value of E_{LUMO} , the more probable that the molecule accepts electrons. According to the E_{LUMO} values, the inhibition efficiency ranking should be: (-Cl) > (-H) > (-NO₂)

The E_{LUMO} ranking shows that the LUMO energy of ph-Cl is the lowest energy. Because this inhibitor contains electron withdrawing group (-Cl), this result enhances the accepting ability of electrons.

The energy gap between HOMO and LUMO is important parameter to determine the theoretical inhibition efficiency [35]. The energy gap is related to softness and hardness. The smaller value ΔE_{GAP} means the more reactivity and higher inhibition efficiency of inhibitors [36-38]. According to the ΔE_{GAP} value, the ranking of inhibitors as follows:



A good agreement is observed between ranking of ΔE_{GAP} values and experimental results.

The dipole moment (μ) provides information on the polarity of the whole molecule. High dipole moment values are reported to facilitate adsorption (and therefore inhibition) by influencing the transport process through the adsorbed layer [39]. Several authors have stated that the inhibition efficiency increases with dipole moments values [40-41]. On the other hand, literature survey reveals that many irregularities appear in the correlation of dipole moments with inhibition efficiency [33, 42]. The dipole moments of (-Cl), (-NO₂) and (-H) are 12.0333D, 10.6634D and 8.8608D, respectively, which are higher than that of H₂O ($\mu = 1.88$ D). The high dipole moment value of these compounds probably indicates strong dipole –dipole interactions between them and metallic surface [43]. Accordingly, the pyrimidothiazine molecules adsorption in aqueous solution can be regarded as a quasi-substitution process of the water molecules by the inhibitors molecules at metal surface (H₂Oads). In addition, the electro negativity parameter (χ) is related to the chemical potential, and higher value of (χ) indicates better. According to the (χ) value, the ranking of inhibitors as follows:

$$(-\text{NO}_2) > (-\text{Cl}) > (-\text{H})$$

Therefore, the highest inhibition efficiency obtained experimentally for (-NO₂) can be explained by the tendency of molecule to receive the electron by S atom in unoccupied orbital (3d). This ability to receive the electron from the metallic surface increases the inhibition efficiency.

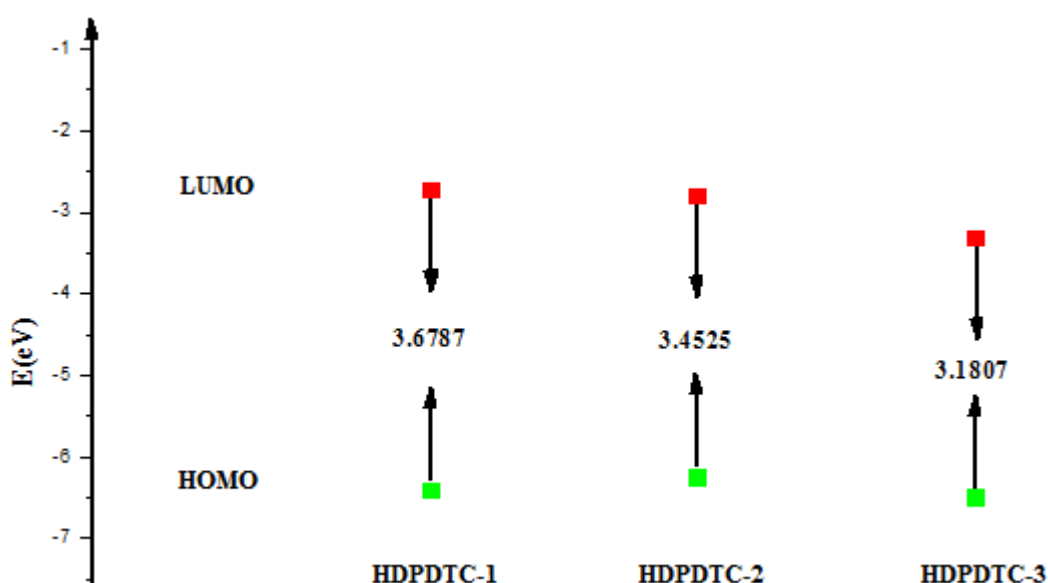


Fig. 11: correlation diagram molecular orbital borders and the gap energy derivatives HDPDTCs compound

Fig. 11 shows the relationship between the molecular frontier orbitals (OMF) pyrimidothiazine compounds studied and their energy gap, HDPDTC-1, HDPDTC-2 and HDPDTC-3 have low energy gap which facilitate their adsorption. The energy of the HOMO orbital is directly related to the ionization potential against by the energy of the LUMO orbital is directly related to the electron affinity. A big difference between the orbital HOMO and LUMO orbital causes high stability of the molecule in chemical reactions. [44] Gece said [45] that the lowest negative value of the HOMO orbital and the lowest energy field (Gap) reflects strong adsorption and high inhibitory efficacy.

CONCLUSION

This work studied of the effect of the synthesized compounds (HDPDTC-1, HDPDTC-2 and HDPDTC-3) as a corrosion inhibitor of carbon steel in 0.1 M HCl medium using EIS, polarization curves, gravimetric measurements and Quantum chemical methods. From the results obtained, the following conclusions can be deduced:

1. All studied organics compounds are highly efficient inhibitors of carbon steel corrosion for the concentrations varying from 10⁻³ to 10⁻⁶ M.
2. These inhibitors were classified as a mixed-type inhibitors of carbon steel corrosion; they affect together cathodic hydrogen reduction reactions and anodic alloy dissolution.
3. The obtained values of ΔG_{ads}^0 at different temperatures indicate that adsorption of studied compounds on the steel surface is spontaneous and favorable dominated by both chemisorption and physisorption mechanism.

4. The adsorption of synthesized compounds on the electrode surface obeyed the Langmuir adsorption isotherm and the high adsorption of these compounds in the range of all concentrations is attributed to the HDPDTC-3.
5. The results of gravimetric, electrochemical impedance spectroscopy and potentiodynamic polarization were in agreement and the ability of inhibition increase with increasing the concentration of the tested inhibitors according to order: HPDTC-3 > HPDTC-2 > HPDTC-1. These results are confirmed with quantum chemical methods.

Acknowledgment

The authors would like to thank MENA NWC for their financial support for grant no: WIF 04. Also, we would like to extend our thanks to Palestine Water Authority (PWA) and MEDRIC for their support. The support given through an "INCRECYT" research contract to M. Zougagh is also acknowledged.

REFERENCES

- [1] B. Mernari, H. El Attari, M. Traisnel, F. Bentiss, M. Lagrenee, *Corros. Sci.* **1988**, 40,391–399.
- [2] G. E. Badr, *Corros. Sci.* **2009**, 51, 2529–2536
- [3] N. A. Negm, A. M. Al Sabagh, M. A. Migahed, H. M. Abdel Bary, H. M. El Din, *Corros. Sci.* **2010**, 52, 2122–2132.
- [4] L. Zeng, G. A. Zhang, X. P. Guo, C. W. Chai, *Corrosion Science* **2015**, 90, 202–215
- [5] R. Yıldız, T. Dogan, I. Dehri, *Corrosion Science* **2014**, 85, 215–221
- [6] M. Hany, Abd El-Lateef, *Corrosion Science* **2015**, 92, 104–117.
- [7] M. A. Hegazy, A. S. El-Tabei, A. H. Bedair, M. A. Sadeq, *Corros. Sci.* **2012**, 54,219–230.
- [8] E. M. Sherif, *Appl. Surf. Sci.* **2014**, 292, 190–196.
- [9] M. Abdallah, *Corros. Sci.* **2002**, 44, 717– 728.
- [10] E. Kowsari, M. Payami, R. Amini, B. Ramezanzadeh, M. Javanbakht, *Taskspecific Appl. Surf. Sci.* 289 (2014) 478–486
- [11] A. S. Fouda, A. S. Ellithy, *corros. sci.* **2009**, 51, 868–875.
- [12] M. J. Bahrami, S. M. A. Hosseini, P. Pilvar, *corros. sci.* **2010**, 52, 2793–2803.
- [13] B. Xu, Y. Liu, X. Yin, W. Yang, Y. Chen, *corros. sci.* **2013**, 74, 206–213.
- [14] H. Serrar, S. Boukhris, A. Hassikou and A. Souizi, *J. Heterocyclic Chem.*, **2013**, DOI 10.1002/jhet.2085
- [15] A. Gaz, F.Ammadi, S. Boukhris, A. Souizi, G. Coudert, *J Heterocycl Chem* **1999**, 5, 413.
- [16] F. Ammadi, S. Boukhris, A. Souizi, Coudert, G. *Tetrahedron Lett* **1999**, 40, 6517.
- [17] Kabanda MM, Murulana LC, Ozcan M, Karadag F, Dehri I, Obot IB, Ebenso EE. *Int JElectrochem Sc* **2012**; 7: 5035–56.
- [18] BD Mert, ME Mert, SG Karda, B.Yazıcı, *Corros Sci* **2011**;53:4265–72.
- [19] AY Musa, AH Kadhun, AB Mohamad, MS Takriff. *Corros Sci* **2010**; 52:3331–40.
- [20] G.Gece, *Corros Sci* **2008**; 50:2981–92.
- [21] MJ Frisch, GW Trucks, HB Schlegel, GE Scuseria, MA Robb, JR Cheeseman Jr.Gaussian03, revision E.01.Walling ford, CT: Gaussian Inc.; **2007**.
- [22] R.G. Pearson, *Inorg. Chem.* 27 (1988) 734.
- [23] V.S. Sastri, J.R. Perumareddi, *Corrosion (NACE)* 53 (1997) 617.
- [24] I. Lukovits, E. Kalman, F. Zucchi, *Corrosion (NACE)* 57 (2001) 3.
- [25] O.L. Riggs, *Corrosion* **1975**, 31, 413–415.
- [26] T. Paskossy, *J. Electroanal. Chem.* **1994**, 364, 111.
- [27] M. Belkhaouda, L. Bammou, R. Salghi, A. Zarrouk, Eno. E. Ebenso, H. Zarrok, B. Hammouti, *Int. J. Electrochem. Sci.*, **2013**, 8, 10987 – 10999.
- [28] A. Dutta, S. Kr. Sahab, P. Banerjee, D. Sukul, *Corrosion Science* **2015**, 98, 541–550.
- [29] H. Zarrok, A. Zarrouk, B. Hammouti, R. Salghi, C. Jama and F. Bentiss, *Corros. Sci.* **2012**, 64 () 643
- [30] A. Yurt, A. Balaban, S.U. Kandemir, G. Bereket, B. Erk, *Mater. Chem. Phys.* **2004**, 85, 420.
- [31] P. Zhao, Q. Liang, Y. Li, *Appl. Surf. Sci.* **2005**, 252, 1596–1607.
- [32] J. Fang, J. Li, *J. Mol. Struct. (Theochem)* **2002**, 593, 179–185.
- [33] G. Bereket, E. Hur, C. Ogretir, *J. Mol. Struct. (Theochem)* **2002**, 578, 79–88.
- [34] A.Y. Musa, A.B. Mohamad, A.A.H. Kadhun, M.S. Takriff, W. Ahmoda, *J. Indus. Eng. Chem.* **2012**, 18, 551–555.
- [35] N. O'zbek, S. Alyar, H. S. Alyar, E. ahin, N. Karacan, *Spectrochim Acta Part A* **2013**; 108:123–32.
- [36] M. O'zcan, I. Dehri , M. Erbil, *Appl Surf Sci* **2004**; 236:155–64.
- [37] AY Musa, RTT Jalgham, AB Mohamad. *Corros Sci* **2012**; 56:176–83.
- [38] F. Zhang, Y. Tang, Z. Cao, W. Jing, Z. Wu, Y. Chen, *Corros Sci* **2012**; 61:1–9.
- [39] A. Popova, M. Christov, T. Deligeorigiev, *Corrosion* **2003**, 59, 756–764.
- [40] M. Sahin, G. Gece, F. Karci, S. Bilgic, *J. Appl. Electrochem.* **2008**, 38, 809–815.
- [41] M.A. Quraishi, R. Sardar, *J. Appl. Electrochem.* **2003**, 33, 1163–1168.

- [42] K.F. Khaled, N.K. Babic-Samardzija, N. Hackerman, *Electrochim. Acta* **2005**, 50, 2515–2520.
[43] K. Ramji, D.R. Cairns, S. Rajeswari, *Appl. Surf. Sci.* **2008**, 254, 4483–4493.
[44] Z. Zhou, R. G. Parr, *J. Am. Chem. Soc.*, **1990**, 112, 5720.
[45] G. Gece, *Corros. Sci.*, **2008**, 50, 2981